Desalination and Water Treatment
www.deswater.com
doi: 10.1080/19443994.2014.958763

56 (2015) 2193–2205
November

Taylor & Francis
Taylor & Francis Group

Adsorption of bromate from emergently polluted raw water using MIEX resin: equilibrium, kinetic, and thermodynamic modeling studies

Lei Ding[a,c,*], Bin Du[b], Gang Luo[a], Huiping Deng[d]

[a]*School of Civil Engineering and Architecture, Anhui University of Technology, Maanshan 243002, P.R. China, Tel. +86 555 2316529; Fax: +86 5552316522; email: dinglei1978@163.com (L. Ding), Tel. +86 13866836552; email: lig1012lg@163.com (G. Luo)*

[b]*School of Energy and Environment, Anhui University of Technology, Maanshan 243002, P.R. China, Tel. +86 18055524059; email: dubin0217@163.com (B. Du)*

[c]*Engineering Research Center of Biomembrane Water Purification and Utilization Technology Ministry of Education, Anhui University of Technology, Maanshanm 243002, P.R. China*

[d]*Key Laboratory of Yangtze River Water Environment, Ministry of Education, Tongji University, Shanghai 200092, P.R. China, Tel. +86 13311875226; email: denghuiping@sina.com (H. Deng)*

Received 3 March 2014; Accepted 19 August 2014

ABSTRACT

This study investigated the kinetics, equilibrium, and thermodynamics of bromate adsorbed on magnetic ion-exchange (MIEX) resin by batch experiments. The pseudo-second-order kinetic model could well describe the adsorption process, and the film diffusion controlled the whole adsorption rate. The Langmuir and Redlich–Peterson isotherm models fitted well the equilibrium data. High removal efficiency of bromate was observed at neutral pH. Other coexistent anions present in raw water affected negatively the removal of bromate significantly. The thermodynamic studies showed the adsorption was a spontaneous thermodynamically, endothermic, and entropy driving process. These analyses on the average free energy, activation energy of adsorption, and quantity changes of bromate and chloride ions in solution before and after adsorption demonstrated that the removal mechanism of bromate adsorbed on MIEX resin was an ion-exchange reaction. Results of the findings suggested that MIEX resin could be utilized effectively to remove bromate from emergently polluted raw water.

Keywords: MIEX resin; Bromate; Equilibrium; Kinetics; Thermodynamics

1. Introduction

Recent years, sudden accidents of water source pollution are on the rise in China [1]. This poses a serious threat to the security of drinking water. Thus, emergency treatment techniques for drinking water are urgent. Bromate (BrO_3^-), as an industrial chemical, is widely used in oxidant and drug synthesis [2]. Hence, a potential sudden pollution of bromate occurs due to abnormal discharge of wastewater and rollover accidents of ship or truck loaded with bromate [3]. Bromate, however, has been defined as a carcinogen of Group 2B by the World Health Organization [4], and limited within 10 ug L^{-1} in potable water [5]. The tradition treatment processes for drinking water, such

*Corresponding author.

as coagulation, sedimentation, filtration, and chlorination, are still used in most waterworks (>95%) in China [6], and aims to remove micro-suspensions, colloid substances, and pathogenic organisms from raw water. But, they are expected to be hardly effective for the removal of bromate because of its existence in anions. Therefore, it is valuable to establish a method for dealing with bromate from suddenly polluted raw water.

Up to now, a series of approaches have been probed for the removal of bromate. Majority of attempts have focused on new materials, such as photocatalytic [7], electrodialysis [8], membrane [9], biological remediation [10], activated carbon [11], and ferrous iron [12]. Obviously, the above methods lack feasibility for removing bromate from suddenly polluted raw water because of short duration and high concentration of bromate [1]. Magnetic ion-exchange (MIEX) resin is a potential candidate as an adsorbent for removing bromate owing to its relatively small particle size (180 μm, 2–5 times smaller than traditional ion-exchange resin), providing much greater external surface area that allows rapid adsorptive removal of pollutant.

MIEX resin, developed jointly by Orica Watercare, Commonwealth Scientific Industrial Research Organization and South Australian Water Corporation [13], is a strong-base anionic resin with chloride as the exchangeable ion [14–17]. In addition, the iron oxide incorporated into the polymer matrix during the preparation process of MIEX resin aids agglomeration and settlement of resin particles after adsorbing pollutants. And these resin particles saturated with pollutants can be effectively regenerated by chloride and can be reused as adsorbent [15,18–20]. These differentiate from the powdered activated carbon that is widely used as adsorbent to remove pollutants from suddenly polluted raw water, but is discharged directly and not regenerated after adsorbing pollutants because of its separation from water difficultly. MIEX resin was mainly used as an adsorbent to eliminate dissolved organics from water and wastewater in previous most studies [21]. Recent years, using MIEX resin to remove inorganic anionic pollutants, such as bromide [13] and phosphate [22], has began to get attention. However, there is a significant gap in knowledge on the removal characteristics of bromate adsorbed on MIEX resin from suddenly polluted raw water. These findings on the adsorption equilibrium, kinetics, and thermodynamics contribute to better understanding the removal mechanism of bromate and designing the reactor.

Accordingly, the goal of this study was to probe the feasibility of using MIEX resin as adsorbent to remove bromate from suddenly polluted raw water. First, adsorption kinetics of bromate on MIEX resin was investigated and the diffusion process of bromate from bulk solution to surface of MIEX resin was analyzed. Second, equilibrium laws of bromate adsorbed on MIEX resin at different temperatures were performed, thermodynamics parameters were calculated, and the thermodynamic feasibility of bromate adsorbed on MIEX resin was discussed. In addition, the effects of solution pH and other anions in solution on the removal of bromate were also studied.

2. Materials and methods

2.1. Materials

2.1.1. Adsorbent

MIEX resin was offered by Beijing Sino-Australia Orica Watercare Technology & Equipment Co. Ltd. Before being used, the virgin MIEX resin was rinsed repeatedly with ultra-pure water to wash away all impurities, and then was stored in ultra-pure water. A certain volume of resin used in adsorption experiments was obtained according to the description in literature [23].

2.1.2. Chemicals and adsorbate

All chemicals used in this study were of GR grade, and purchased from Sinopharm Chemical Reagent Co. Ltd, China. Sodium bromate ($NaBrO_3$) was defined as adsorbate in this study. A precise stock solution of bromate (BrO_3^-, 1,000 mg L^{-1}) was prepared by dissolving accurately weighed sample of sodium bromate in ultra-pure water. Samples used in adsorption experiments were obtained by diluting standard stock solution with distilled water where needed.

2.2. Methods

2.2.1. Kinetic study

Kinetic experiments of bromate adsorbed on MIEX resin were carried out at different bromate concentrations (5, 10 mg L^{-1}) and different solution temperatures (283, 293, and 303 K) by static batch adsorption, respectively. Taking the experiment of 5 mg L^{-1} bromate adsorbed on MIEX resin as an example illustrated the adsorption process is as follows: First, 0.2 mL MIEX resin was added into a serious of beakers containing 500 mL bromate solution with the concentration of 5 mg L^{-1}, respectively. Then, these beakers were sealed with aluminum foil and kept on a set of digital display stable temperature magnetic

stirrer. These solutions were mixed with a constant speed of 150 rpm at 288 K. These samples were taken down at preset time intervals and filtered rapidly using a 0.45 μm Millipore membrane filter, respectively. The bromate concentrations in filtrates were measured by a Shimadu Ion Chromatograph. Under those conditions of 10 mg L^{-1} bromate concentration and different solution temperatures (283, 293, and 303 K), the similar kinetic experiments were conducted. In those experiments, the pH values of bromate solutions were kept originally without any adjustment. All experiments were carried out in triplicate and average values were reported herein.

The amount of bromate adsorbed on MIEX resin at time t, q_t (mg, mL^{-1}), was calculated using mass balance relationship [24]:

$$q_t = \frac{(c_0 - c_t)V}{W} \tag{1}$$

where C_0 and C_t were liquid-phase concentration of BrO_3^- (mg L^{-1}) at initial and time t, respectively. V(L) was the volume of solution and W (mL) represented the volume of adsorbent used.

In order to better understand the mechanism of adsorption, pseudo-first-order, pseudo-second-order, and Elovich models were applied to analyze the kinetic process of bromate adsorbed on MIEX resin, respectively. For kinetic models above, the equations were conveyed as follows [13]:

$$\text{Pseudo-first-order model} : \ln(q_e - q_t) = \ln q_e - k_1 t \tag{2}$$

$$\text{Pseudo-second-order model} : \frac{t}{q_t} = \frac{1}{k_2 q_e^2} + \frac{t}{q_e} \tag{3}$$

$$\text{Elovich model} : q_t = \frac{1}{\beta}\ln(1 + \partial\beta t) \tag{4}$$

where q_e, (mg mL^{-1}), was the amount of bromate adsorbed on MIEX resin at equilibrium; t (min), was adsorption time; k_1 (min^{-1}) and k_2 (mL mg^{-1} min^{-1}) were the rate constants of pseudo-first-order and pseudo-second-order, respectively; α (mg mL^{-1} min^{-1}) was the initial adsorption rate constant; and β (mL mg^{-1}) was related to the extent of surface coverage and activation energy for chemisorptions.

In addition, the intra-particle diffusion model (described by Eq. (5)) was used to investigate the particularly potential rate-controlling step and the transient behavior of adsorbing bromate process from aqueous solution to MIEX surface, which was explained as follows [13]:

$$\text{Intra-particle diffusion model} : q_t = k_{id} t^{\frac{1}{2}} + c_i \tag{5}$$

where k_{id} (mg mL^{-1} $min^{-1/2}$) was the intra-particle diffusion rate constant and c_i was a constant.

The Boyd model (expressed by Eq. (6)) was selected to predict the actual slow step involved in the process of bromate adsorbed on MIEX resin.

$$\text{Boyd model} : Bt = -0.4977 - \ln\left(1 - \frac{q_t}{q_e}\right) \tag{6}$$

where B was a constant.

2.2.2. Isotherm study

Static equilibrium trials of bromate adsorbed on MIEX resin were conducted at 283, 293, and 303 K. Equilibrium adsorption at 283 K was taken as an example to describe the experimental method. 0.2 mL MIEX resin was added into a set of beakers containing 500 mL solutions with various bromate concentrations (1, 2, 3, 4, 5, and 6 mg L^{-1}), respectively. These slurries were mixed on the digital display stable temperature stirrer with a constant agitation speed of 150 rpm for 2 h (the pre-studies showed adsorption of bromate on MIEX resin could reach equilibrium after 90 min) at 283 K. Then, resin particles were separated using a 0.45 um Millipore membrane filter, and the bromate concentrations in filtrates were analyzed. During these experimental processes, pH values of bromate solutions were kept originally without any adjustment. The similar equilibrium adsorption tests at 293 and 303 K were conducted.

The amount of bromate adsorbed on MIEX resin at equilibrium, q_e (mg mL^{-1}) was calculated by the following equation:

$$q_e = \frac{(C_0 - C_e)V}{W} \tag{7}$$

where C_e (mg L^{-1}) was the bromate concentration in liquid phase at equilibrium.

Langmuir, Freundlich, and Redlich–Peterson isotherm models were applied to fit these equilibrium data in this study, respectively.

The nonlinear forms of above isotherm models were as follows [25]:

$$\text{Langmuir isotherm} : \frac{C_e}{q_e} = \frac{C_e}{q_{\max}} + \frac{1}{q_{\max} b} \tag{8}$$

$$\text{Freundlich isotherm}: \log q_e = \frac{1}{n}\log C_e + \log k_f \quad (9)$$

$$\text{Redlich–Peterson isotherm}: q_e = \frac{K_R C_e}{1 + \alpha_R C_e^b} \quad (10)$$

where q_{max} (mg mL^{-1}) was the theoretical maximum monolayer adsorption capacity of adsorbent; b (L mg^{-1}) was the Langmuir constant; k_f (mg mL^{-1} (L $mg^{-1})^{1/n}$) was the Freundlich constant related to the bonding energy and adsorption capacity, and $1/n$ was the heterogeneity factor; K_R, α_R, and b were the constants of Redlich–Peterson isotherm model.

D–R isotherm model was described by Eqs. (11)–(13), and used to calculate the average free energy during the process of bromate adsorbed on MIEX resin.

$$\text{D–R isotherm model}: q_e = q_{max}\exp(-B_{DR}\zeta^2) \quad (11)$$

$$\zeta = RT\ln\left(1 + \frac{1}{C_e}\right) \quad (12)$$

$$E = \frac{1}{\sqrt{2B_{DR}}} \quad (13)$$

where B_{DR} (mol^2/J^2) and ζ (kJ) were the D–R model constant and the Polanyi potential, respectively; R (8.314 J mol^{-1} K^{-1}) was the ideal gas constant; T (K) was solution temperature; E (J/mol) was the average free energy.

2.2.3. Effect of solution pH and anions on bromate removal

Batch adsorption experiments were employed to investigate the effects of initial solution pH on bromate removal. Adsorption procedure comprised the following steps: (a) transfer 500 mL bromate solution with the concentration of 5 mg L^{-1} into a set of beakers, respectively, and adjust the pH values to 6, 7, 8, and 9 (pH of raw water usually ranges 6–9) with 0.1 M HCl or 0.1 M NaOH solutions; (b) 0.2 mL MIEX resin was added into bromate solutions above, respectively, and these mixtures were agitated on the digital display stable temperature stirrer with a constant agitation speed of 150 rpm at 285 K for 2 h; (c) after adsorption, the bromate concentrations in filtrates were analyzed and the amounts of bromate adsorbed on MIEX resin were calculated. All the experiments were executed in triplicate and the average values were given.

Batch adsorption experiments were also conducted to investigate the effects of different types of anions on the removal of bromate on MIEX resin by adding chloride, sulfate, and bicarbonate with the equivalent concentration of 1 meq L^{-1} into bromate solutions with the concentration of 5 mg L^{-1}, respectively. The experimental process was similar to that of effects of solution pH on bromate removal.

2.2.4. Thermodynamic study

Adsorption thermodynamics focused on the energy change of adsorption process, which was significant to obtain the thermodynamic property of adsorption behavior. Three thermodynamic parameters, standard Gibbs free energy change (ΔG°, kJ mol^{-1}), standard enthalpy change (ΔH°, kJ mol^{-1}), and standard entropy change (ΔS°, J mol^{-1} k^{-1}), were calculated to evaluate thermodynamic feasibility and spontaneous nature of bromate adsorbed on MIEX resin in this study.

These parameters can be obtained from the following equations [26]:

$$K_{eq} = \frac{C_{ad,e}}{C_e} \quad (14)$$

$$\ln K_{eq} = \frac{\Delta S^\circ}{R} - \frac{\Delta H^\circ}{RT} \quad (15)$$

$$\Delta G^\circ = \Delta H^\circ - T\Delta S^\circ \quad (16)$$

where K_{eq} (L mL^{-1}) was the distribution coefficient and $C_{ad,e}$ (mg mL^{-1}) was the equilibrium adsorption capacity of bromate on MIEX resin at different temperatures.

The adsorption activation energy during the process of bromate adsorbed on MIEX resin was calculated by the Arrhenius equation described as follows [26]:

$$\ln k_2 = \ln A - \frac{E_a}{RT} \quad (17)$$

where A was the Arrhenius factor and E_a (kJ/mol) was the activation energy of adsorption.

2.2.5. Determination of bromate

Bromate was measured using suppressed conductivity detection on a Shimadu Ion Chromatograph (Shimadu, Japan) with an IC SI-52G guard column

(4.6 mm × 10 mm, Shodex, Japan) and an IC SI-52 4E analytical column. (4.0 mm × 250 mm, Shodex, Japan). The 3.6 mM sodium carbonate (Na_2CO_3) was used as a solvent and the flow rate of the solvent was 0.8 mL min^{-1} with a sample injection volume of 20 μL. The temperature of the column and detector compartment was set to 45°C.

3. Results and discussion

3.1. Adsorption kinetics

3.1.1. Effect of adsorption time and initial bromate concentration

With the target to capture the equilibrium time for maximum uptake, bromate adsorbed on MIEX resin was researched as a function of adsorption time with different bromate concentrations. And the results were shown in Fig. 1.

At the initial stage of adsorption, before 20 min, the uptake of bromate adsorbed on MIEX resin mushroomed with increasing adsorption time. This was because generous unused active adsorption sites on MIEX resin surface swiftly adsorbed bromate from aqueous solutions. During the subsequent period of 20–40 min, it showed a slow rise in uptake of bromate. This was attributed to the fact that it was difficult for those vacant adsorption sites to be occupied by bromate in bulk solution due to the repulsion of bromate between in bulk solution and on the resin surface [23]. After adsorption of 40 min, the uptake of bromate kept a constant approximately with increasing adsorption time. This implied that the adsorption of bromate on MIEX resin reached an equilibrium at 40 min. Compared to the conventional adsorbents used to remove bromate, such as granular activated carbons and powdered activated carbons (the time required to reach adsorption equilibrium was from 4 to 20 h [27–29]), MIEX resin adsorbing bromate from aqueous solution was a fast kinetic process. Based on the fact, MIEX resin can be used as a candidate adsorbent to remove bromate from emergently polluted raw water.

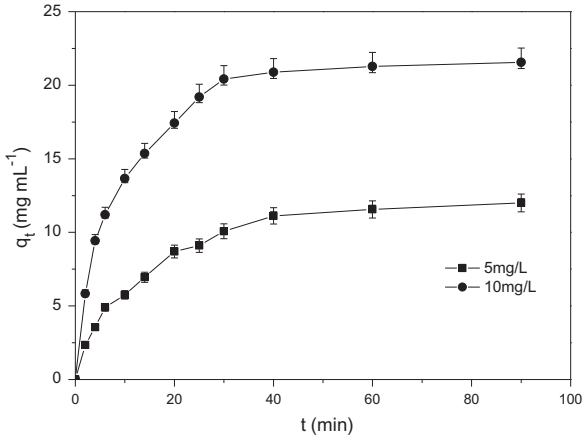

Fig. 1. Effects of adsorption time and initial bromate concentration on the removal of bromate on MIEX resin.

In addition, as shown in Fig. 1, for an identical adsorption time t, the uptake of bromate adsorbed on MIEX resin increased with increasing the initial bromate concentration from 5 to 10 mg L^{-1}. This was explained that when bromate concentration was higher, the greater concentration gradient enabled bromate settle into the internal pores of resin, and those active adsorption sites were made use of fully [12]. This was similar to the result of Bhatnagar using granular ferric hydroxide to remove bromate from water [30].

3.1.2. Kinetic model of bromate adsorbed on MIEX resin

Pseudo-first-order, pseudo-second-order, and Elovich models were used to fit the experimental data at different initial bromate concentrations, respectively. The results were provided in Table 1. The fitted curves were given in Fig. 2 with experimental results.

From Table 1, compared to the pseudo-first-order and Elovich models, the correlation coefficients (R^2) of pseudo-second-order model are the biggest, and the standard errors (SE) were the smallest. In addition, Fig. 2 showed that these curves fitted by the pseudo-second-order model were perfectly close to the experimental results. Accordingly, the pseudo-second-order model was the most suitable to describe the kinetic process of bromate adsorbed on MIEX resin. This suggested the kinetic process was mainly controlled by the chemisorptions which involved chemical bonding between bromate ion and MIEX resin [31].

For pseudo-second-order model, the initial adsorption rate, h (mg mL^{-1} min^{-1}), was expressed by the following equation:

$$h = k_2 q_e^2 \tag{18}$$

Table 1 demonstrated that these values of h increased from 0.082 to 0.152 with increasing bromate concentration from 5 to 10 mg L^{-1}. This showed that initial rate of bromate adsorbed on MIEX resin increased obviously at higher bromate concentration. It agreed with the results of Fig. 1 demonstrating it was likely due to the fact that high bromate concentration accelerated the diffusion process of bromate from bulk solution to solid phase [13].

Table 1
Kinetic parameters of bromate adsorbed on MIEX resin at different bromate concentrations

Pseudo-first-order							
C_0 (mg L^{-1})	q_e (exp) (mg mL^{-1})	q_e (cal) (mg mL^{-1})	k_1 (min^{-1})		R^2	SSE	SE
5	12	11.64	0.0716		0.9832	2.5641	0.5338
10	21.56	20.75	0.1174		0.977	10.9691	1.104
Pseudo-second-order							
C_0 (mg L^{-1})	q_e (exp) (mg mL^{-1})	q_e (cal) (mg mL^{-1})	k_2 (mg mL^{-1} min^{-1})	h	R^2	SSE	SE
5	12	13.89	0.0059	0.082	0.9926	1.1335	0.3549
10	21.56	23.74	0.0064	0.152	0.9933	3.1864	0.595
Elovich model							
C_0 (mg L^{-1})	A (mg mL^{-1} min^{-1})	β (mL mg^{-1})			R^2	SSE	SE
5	1.88	0.31			0.9837	2.4905	0.526
10	8.27	0.21			0.9728	12.965	1.2002

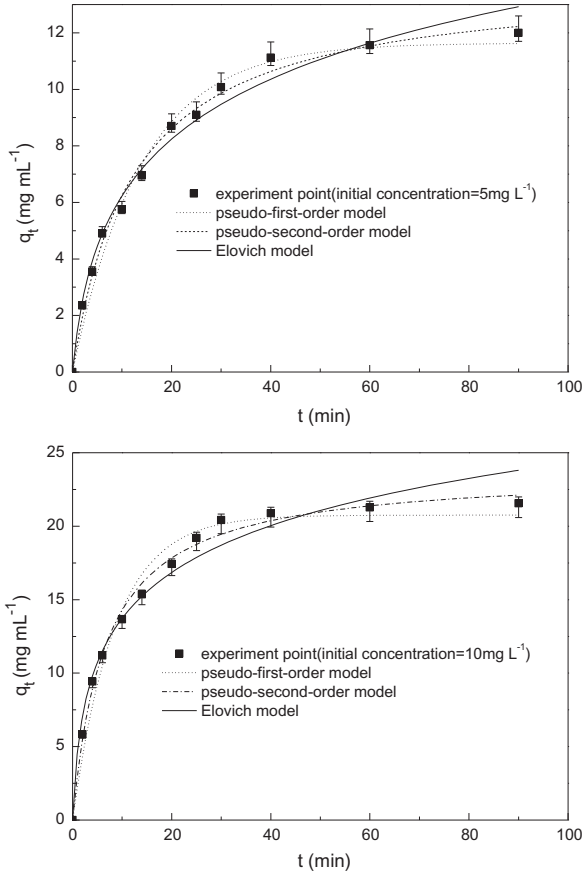

Fig. 2. The fitted curves of adsorption kinetics of bromate on MIEX resin.

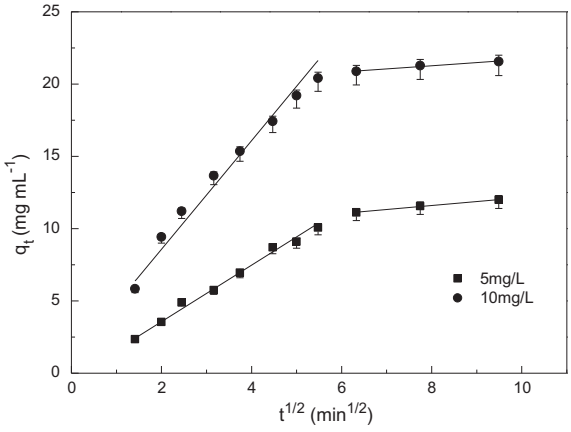

Fig. 3. Plots of intra-particle diffusion model for the adsorption of bromate on MIEX resin at different initial bromate concentrations.

3.1.3. Diffusion mechanism of bromate

The intra-particle diffusion model was used to analyze the diffusion mechanism of bromate from bulk solution to surface of MIEX resin at different initial bromate concentration. Fig. 3 expressed the relationship of q_t vs. $t^{1/2}$ at different initial bromate concentrations. Table 2 involved linear regression parameters (k_{id}, c_i) and correlation coefficients (R^2).

Fig. 3 conveyed that it was not a linear relationship of q_t vs. $t^{1/2}$ within the whole adsorption time. This implied the adsorption process of bromate on MIEX resin did not agree with the intra-particle model within whole adsorption time. For the different initial bromate concentrations, however, each plot could be divided into two segments. And Table 2 showed that each segment was linear with high correlation coefficients ($R^2 > 0.95$), indicating intra-particle diffusion occurred within corresponding adsorption time range. However, the values of C_i (i = 1 or 2 given in Table 2) were beyond 0. This showed each segment that did not pass through the origin implied that intra-particle diffusion was not the only rate-limiting step, probably involving other processes, such as film diffusion [23].

Table 2
Constants and correlation coefficients of intra-particle diffusion model for bromate adsorption on MIEX resin

	Intra-particle diffusion model					
C_0 (mg L^{-1})	K_{id1} (mg mL^{-1} $min^{-1/2}$)	C_1	R^2	K_{id2} (mg mL^{-1} $min^{-1/2}$)	C_2	R^2
5	1.885	0.108	0.9907	0.277	9.382	0.9932
10	3.414	2.239	0.9815	0.215	19.549	0.9550

Boyd model was used to further fit the kinetic data at different initial bromate concentrations in order to predict the actual low step during the process of bromate adsorbed on MIEX resin [32]. The values of Bt were calculated by Eq. (6), and Fig. 4 reflected the Boyd plots of Bt vs. *t*.

It was observed from Fig. 4 that Boyd plots gave well-linear forms at different initial bromate concentrations, but they did not pass through the origin. This implied that the adsorption process of bromate on MIEX resin was controlled by liquid-film diffusion [32].

The values of B were obtained from the slopes of linear of Bt against t at different initial bromate concentrations. With bromate concentration increasing from 5 to 10 mg L^{-1}, the values of B increased from 0.055 to 0.072. These values of *B* were far less than 1, further verifying the fact that the adsorption of bromate on MIEX was controlled by the film diffusion [33].

3.2. Equilibrium of bromate adsorbed on MIEX resin

3.2.1. Adsorption equilibrium

Equilibrium experiments of bromate adsorbed on MIEX resin were conducted at 283, 293, and 303 K in order to evaluate the potential of using MIEX resin to remove bromate from raw water. The results were given in Fig. 5.

Fig. 5 showed that MIEX resin could effectively remove bromate from aqueous solutions, and raising temperature of solution facilitated the growth in equilibrium capacity of bromate adsorbed on MIEX resin. This demonstrated that bromate ions were easy to be removed from aqueous solution at higher temperature of solution, and implied that the adsorption might be an endothermic process.

3.2.2. Isotherm model of bromate adsorbed on MIEX resin

Langmuir, Freundlich, and Redlich–Peterson isotherm models were used to fit the equilibrium adsorption data at different solution temperatures, respectively. Table 3 listed model constants, correlation coefficients, and SE. The fitted curves were plotted with experimental results in Fig. 6.

As seen in Table 3, compared to the Freundlich model, Langmuir and Redlich–Peterson models gave good fittings with higher correlation coefficients ($R^2 > 0.99$) and lower values of SE. It was clear from Fig. 6 that the curves fitted by Langmuir and

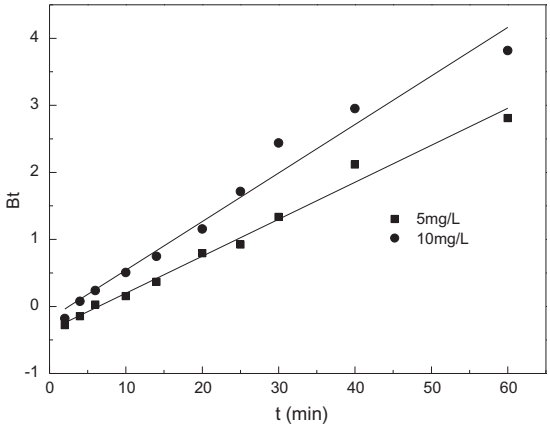

Fig. 4. Boyd plots of bromate adsorbed on MIEX resin.

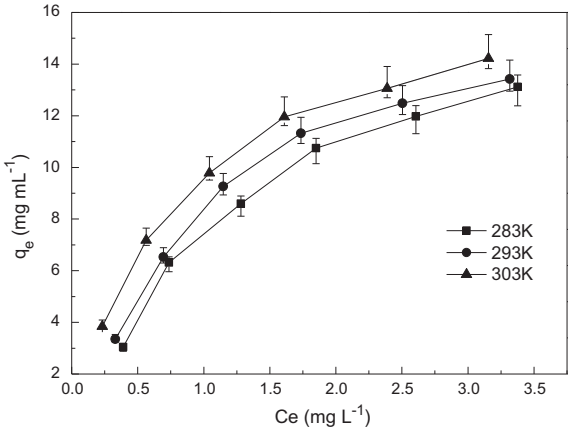

Fig. 5. Adsorption equilibrium of bromate on MIEX resin at 283, 293, and 303 K.

Table 3
Constants, correlation coefficients, SEE, and SE of Langmuir, Freundlich, and Redlich−Peterson isotherm models

Langmuir model						
Temperature	q_{max} (mg mL^{-1})	b (L mg^{-1})		R^2	SSE	SE
283	20.02	0.584		0.988	0.69	0.415
293	19.04	0.772		0.9894	0.629	0.397
303	17.97	1.175		0.9985	0.092	0.152
Freundlich model						
Temperature	k_f	$1/n$		R^2	SSE	SE
283	7.113	0.542		0.9501	2.862	0.846
293	7.904	0.491		0.93	3.769	0.971
303	9.063	0.428		0.9609	2.404	0.775
Redlich–Peterson model						
Temperature	K_{RP}	A_{RP}	b	R^2	SSE	SE
283	9.574	0.291	1.338	0.9906	0.403	0.366
293	11.358	0.35	1.38	0.9981	0.085	0.169
303	21.124	1.177	0.999	0.998	0.092	0.175

Redlich−Peterson models were also closer to the experimental values than those fitted by the Freundlich model. These showed that Langmuir and Redlich−Peterson isotherm models could well describe the adsorption equilibrium of bromate on MIEX resin. This result was coincident with usual opinion that adsorption equilibrium of pollutants on ion-exchange resin agreed with Langmuir isotherm model [34].

3.2.3. Comparison with other adsorbents

Adsorption performances of different adsorbents can be evaluated by the parameter of maximum adsorption capacity (q_{max}) obtained from Langmuir isotherm model. Table 4 listed q_{max} and time needed to reach equilibrium using various adsorbents to remove bromate from water [12,30,35–38]. Compared to other adsorbents, MIEX resin had decided advantages with higher adsorption capacity (125.10 mg g^{-1}) and shorter time needed for reaching adsorption equilibrium. Thus, MIEX resin had a marvelous potential for removing bromate from raw water.

3.3. Effect of initial pH of solution

The effects of initial pH of solution on bromate removal were shown in Fig. 7. Although the uptakes of bromate adsorbed on MIEX resin decreased slightly with increasing initial pH of solution from 6.00 to 7.00, the higher uptakes were still kept on. The isoelectric point of MIEX resin was 6.07. Therefore, the surfaces of resin were charged negatively at pH 7.00. The electrostatic repulsion between surface of resin and bromate ions made it difficult that bromate ions were adsorbed on resin [39]. This might be a reason that the uptake of bromate decreased slightly. With further increasing pH to 9, the uptake of bromate declined rapidly. This was due to the fact that the hydroxide ions competed for adsorption sites with bromate ions at strong alkali.

3.4. Effect of coexistent anions

The effects of other anions (such as chloride, bicarbonate, and sulfate) on the removal of bromate adsorbed on MIEX resin were plotted in Fig. 8. The removal efficiency of bromate decreased from 85.40 to 22.33, 22.40, and 5.47% with the addition of chloride, bicarbonate, and sulfate with an identical concentration of 1 meq L^{-1}, respectively. This showed that other anions in raw water affected negatively the removal of bromate because of competing for adsorption sites with bromate ions. Compared with the chloride and bicarbonate, the affinity of divalent sulfate to activated sites was much more than that of the monovalent chloride, resulting in the more serious decrease in uptake of bromate.

3.5. Adsorption thermodynamic

3.5.1. Thermodynamic parameters of bromate adsorbed on MIEX resin

For the equilibrium adsorption data at different temperatures, the solid–liquid distribution coefficients (K_{eq}) of bromate adsorbed on MIEX resin were calculated by the Eq. (14), and these straight lines of ln(K_{eq}) against 1,000/T were plotted in Fig. 9. The thermodynamic parameters, ΔH° and ΔS°, were obtained from

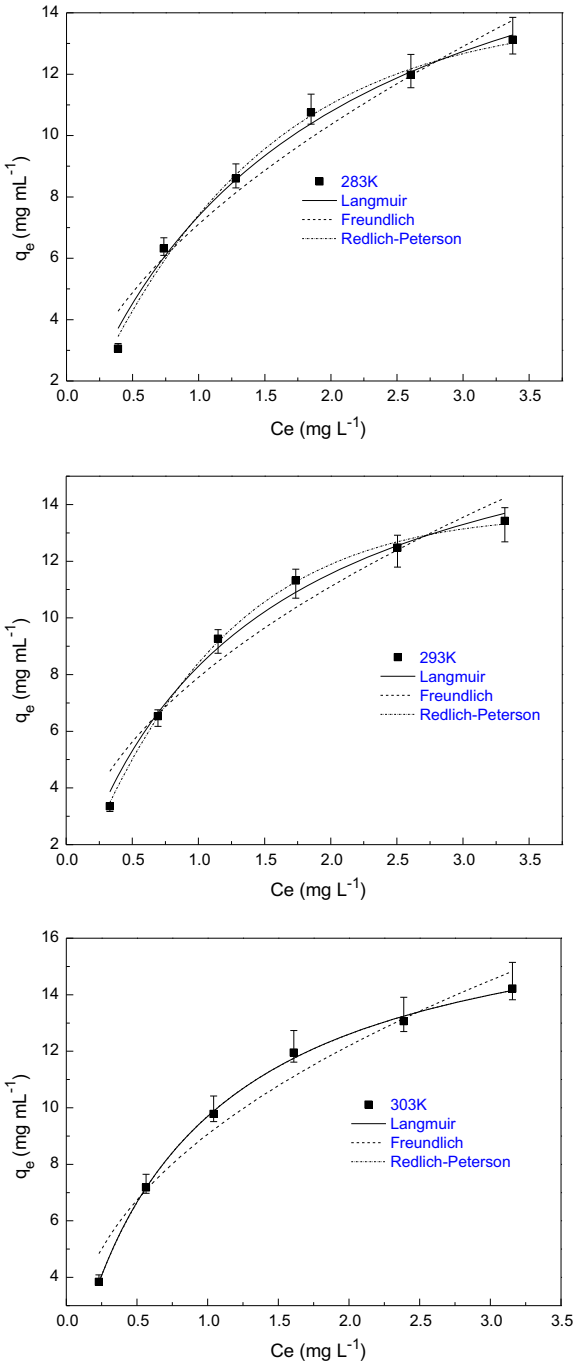

Fig. 6. Comparison between experimental data and predicted values of adsorption equilibrium of bromate on MIEX resin at 283, 293, and 303 K.

the slopes and intercepts of these straight lines. Then the values of ΔG° at different temperatures were calculated by the Eq. (16), and these results were shown in Table 5.

All the values of ΔG° were negative, indicating that the adsorption of bromate on MIEX resin was thermodynamically spontaneous. And further more, the values of ΔG° became more negative with raising temperature, implying the process of bromate adsorbed on MIEX resin was easier to occur at high temperature of solution. The positive values of ΔH° showed the adsorption process was endothermic. The positive values of ΔS° showed that the degree of disorder on the solid–liquid interface increased after adsorption, demonstrating good affinity of MIEX resin for bromate [30].

3.5.2. Average free energy of bromate adsorbed on MIEX resin

Average free energy of adsorption (E, kJ mol^{-1}) obtained from Dubinin–Radushkevich isotherm model can be used to judge adsorption type. The Dubinin–Radushkevich isotherm model was used to fit the equilibrium adsorption data at 283, 293, and 303 K. The values of B_{DR} at different temperatures were listed in Table 6. The values of E were calculated by the Eqs. (11)–(13) and also listed in Table 6. It was observed from Table 6 that the values of average free energy of bromate adsorbed on MIEX resin at different temperatures were all above 8 kJ mol^{-1}, indicating that the adsorption was a chemical sorption process including an ion-exchange reaction [40].

3.5.3. Activation energy of bromate adsorbed on MIEX resin

Activation energy of adsorption (E_a, kJ mol^{-1}) was also used to judge adsorption type. The adsorption kinetics of bromate on MIEX resin at 283, 293, and 303 K were conducted in order to calculate the activation energy of adsorption. The pseudo-second-order kinetic model was used to fit the kinetic data of different temperatures, and the results were given in Table 7. Based on Eq. (17), the plot of $\ln(k_2)$ vs. $1/T$ was a straight line (Fig. 10). The value of E_a was obtained from the slope. The activation energy of bromate adsorbed on MIEX was 31.8 kJ mol^{-1}, indicating the adsorption was a chemical sorption process [41]. This was consistent with the conclusion obtained from the average free energy of adsorption.

3.6. Removal mechanism of bromate on MIEX resin

For the equilibrium adsorption data at 293 K, the quantity changes of bromate and chloride ions in solutions before and after adsorption were calculated in

Table 4
Comparison of bromate removal with various adsorbents

Adsorbents	Adsorption equilibrium time t	Max capacity q_{max} (mg/g)	Bibliography
Nanocoated quartz sand	10 min	0.05	[12]
Granular $Fe(OH)_3$	60 min	17.86	[27]
GAC	24 h	7.2	[32]
Nano Al_2O_3	2 h	6.66	[33]
Amorphous aluminum hydroxide	24 h	5.12	[34]
PAC	24 h	99.6	[35]
MIEX resin	40 min	125.1	This study

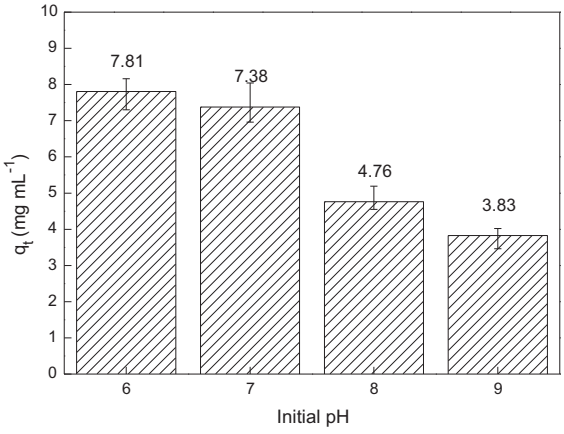

Fig. 7. Effect of pH value on the bromate adsorption on MIEX resin.

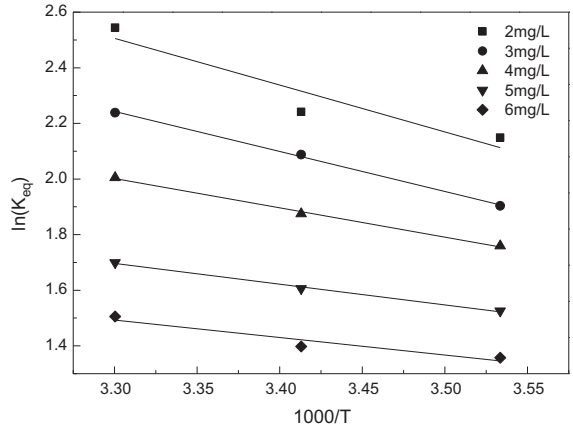

Fig. 9. Plots of ln (K_{eq}) vs. 1,000/T for the adsorption of bromate on MIEX resin.

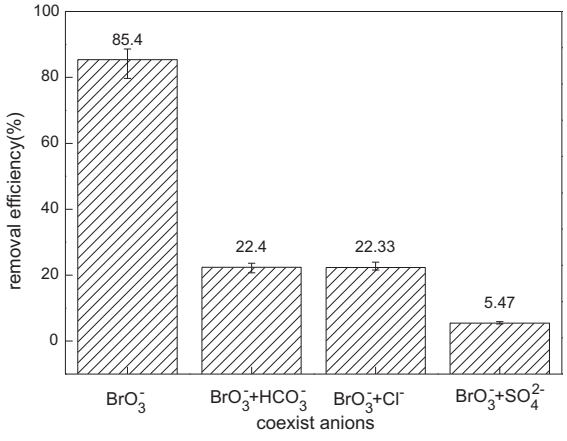

Fig. 8. Effect of inorganic anions on the bromate adsorption on MIEX resin.

Table 5
Thermodynamic parameters of bromate adsorption on MIEX resin

C_0 mg L^{-1}	ΔH° kJ mol^{-1}	ΔS° J/(mol K^{-1})	ΔG° (kJ mol^{-1})		
			283 K	293 K	303 K
2	13.991	67.006	−4.302	−5.642	−6.312
3	11.950	58.080	−3.906	−5.068	−5.649
4	8.742	45.489	−3.676	−4.586	−5.041
5	6.185	34.514	−3.237	−3.927	−4.272
6	5.243	29.721	−2.871	−3.465	−3.762

order to further explore the removal mechanism of bromate on MIEX resin. And the results were shown in Fig. 11. Fig. 11 demonstrated that the bromate ions which were adsorbed on MIEX resin were roughly equivalent to the chloride ions which were released from resin surface into aqueous solution. It was proved that the removal mechanism of bromate adsorbed on MIEX resin was an ion-exchange reaction, agreeing with the conclusion obtained from the energy analysis.

Table 6
Mean adsorption energy of bromate on MIEX resin

T (K)	B_{DR}	E (kJ mol^{-1})	R^2
283	7.06E-09	8.416	0.9729
293	6.21E-09	8.972	0.9782
303	4.58E-09	10.452	0.9499

Table 7
The results fitted by the pseudo-second-order kinetics model at 283, 293, and 303 K

T (K)	q_{max} (mg mL^{-1})	k_2 (mg mL^{-1} min^{-1})	R^2
283	10.05	0.0096	0.9906
293	9.97	0.0121	0.9879
303	9.80	0.0235	0.9777

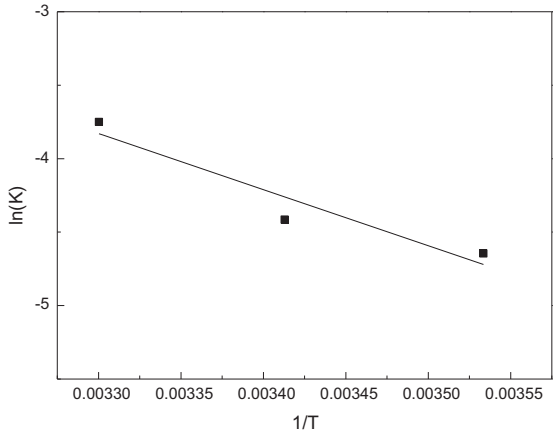

Fig. 10. The plot of calculating the activation energy for the bromate adsorption on MIEX resin.

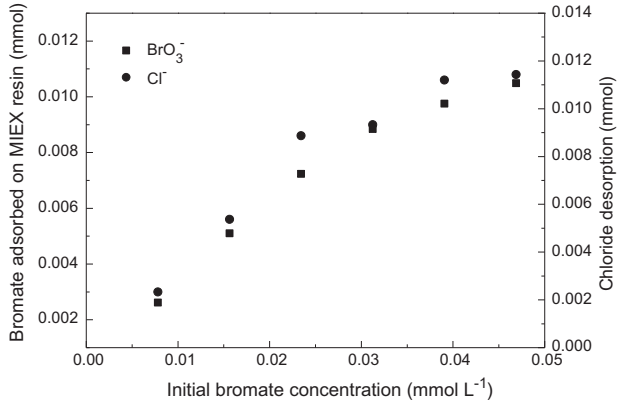

Fig. 11. Quantitative analysis of bromate ions adsorbed on MIEX resin and chloride ions in solution at adsorption equilibrium.

4. Conclusion

Present studies showed that MIEX resin had a marvelous potential to be used as adsorbent for removing bromate from emergently polluted raw water. The adsorption of bromate on MIEX resin was a quick process, and the equilibrium was reached after adsorption of 40 min. The Langmuir and Redlich–Peterson isotherm models fitted well the equilibrium data with a maximum adsorption capacity of 125.10 mg g^{-1}. The pseudo-second-order kinetic model could well describe the kinetic process, and the film diffusion controlled the whole adsorption rate. High removal efficiency of bromate was observed at pH 6–7. Other coexistent anions affected negatively the removal of bromate significantly. The adsorption was a spontaneous thermodynamic, endothermic and entropy-driving process. The removal mechanism of bromate adsorbed on MIEX resin was an ion-exchange reaction.

Acknowledgments

This work was supported by the National Natural Science Foundation of China (grant number 51308001), the Innovation Research Funds of the Anhui University of Technology for Graduate (2012038), project supported by the special funds of the Anhui University of Technology innovation education of College Students (2013018Y), the Innovation Research Funds of the Anhui University of Technology for Graduate (2013032).

List of symbols

C_0 — liquid-phase concentration at initial (mg L^{-1})
C_t — liquid-phase concentration at time t (mg L^{-1})
C_e — equilibrium concentration (mg L^{-1})
q_e — amount of bromate adsorbed at equilibrium (mg mL^{-1})
q_t — amount of bromate adsorbed at time t (mg mL^{-1})
α — initial adsorption rate constant (mg mL^{-1} min^{-1})
β — relating to chemisorptions (mL mg^{-1})
k_{id} — intra-particle diffusion rate constant (mg mL^{-1} min$^{-1/2}$)
q_{max} — theoretical maximum adsorption capacity (mg mL^{-1})
b — langmuir adsorption constant (1 mg^{-1})
k_f — freundlich adsorption constant (mg mL^{-1}(L mg^{-1})$^{1/n}$)
K_R — redlich–Peterson adsorption constant
B_{DR} — D–R model constant (mol^2/J^2)
ζ — polanyi potential (kJ)
T — solution temperature (°C, K)
E — average free energy (J/mol)

K_{eq} — distribution coefficient (L mL^{-1})
A — arrhenius factor
E_a — activation energy of adsorption
ΔG° — standard free energy change (kJ mol^{-1})
ΔH° — enthalpy change (kJ mol^{-1})
ΔS° — entropy change (kJ mol^{-1})

References

[1] C.L. Dai, B.M. Chi, Z.P. Liu, City's emergency water source field in North China with the example of Changchun City, Procedia Environ. Sci. 12 (2012) 474–483.

[2] D. Tomalik-Scharte, D. Maiter, J. Kirchheiner, H.E. Ivison, U. Fuhr, W. Arlt, Impaired hepatic drug and steroid metabolism in congenital adrenal hyperplasia due to P450 oxidoreductase deficiency, Eur. J. Endocrinol. 163 (2010) 919–924.

[3] H. Jian, C. Junying, L. Jiahong, Q. Dayong, Risk identification of sudden water pollution on fuzzy fault tree in beibu-gulf economic zone, Procedia Environ. Sci. 10 (2011) 2413–2419.

[4] M.A. Shannon, P.W. Bohn, M. Elimelech, J.G. Georgiadis, B.J. Mariñas, A.M. Mayes, Science and technology for water purification in the coming decades, Nature 452 (2008) 301–310.

[5] C. Gong, Z. Zhang, Q. Qian, D. Liu, Y. Cheng, G. Yuan, Removal of bromide from water by adsorption on silver-loaded porous carbon spheres to prevent bromate formation, Chem. Eng. J. 218 (2013) 333–340.

[6] Y.P. Zhang, Y.L. Yang, Y. Zhang, T.Q. Zhang, M.M. Ye, Heterogeneous oxidation of naproxen in the presence of α-MnO2 nanostructures with different morphologies, Appl. Catal., B 127 (2012) 182–189.

[7] M. Sturini, E. Rivagli, F. Maraschi, A. Speltini, A. Profumo, A. Albini, Photocatalytic reduction of vanadium(V) in TiO_2 suspension: Chemometric optimization and application to wastewaters, J. Hazard. Mater. 254–255 (2013) 179–184.

[8] J.A. Wiśniewski, M. Kabsch-Korbutowicz, S. Łakomska, Donnan dialysis and electrodialysis as viable options for removing bromates from natural water, Desalination 281 (2011) 257–262.

[9] S. Kliber, J.A. Wiśniewski, Removal of bromate and associated anions from water by Donnan dialysis with anion-exchange membrane, Desalin. Water Treat. 35 (2011) 158–163.

[10] L. Xie, C. Shang, Effects of copper and palladium on the reduction of bromate by Fe(0), Chemosphere 64 (2006) 919–930.

[11] M. Siddiqui, W. Zhai, G. Amy, C. Mysore, Bromate ion removal by activated carbon, Water Res. 30 (1996) 1651–1660.

[12] C.H. Xu, J.J. Shi, W.Z. Zhou, B.Y. Gao, Q.Y. Yue, X.H. Wang, Bromate removal from aqueous solutions by nano crystalline akaganeite (β-FeOOH)-coated quartz sand (CACQS), Chem. Eng. J. 187 (2012) 63–68.

[13] L. Ding, H.P. Deng, C. Wu, X. Han, Affecting factors, equilibrium, kinetics and thermodynamics of bromide removal from aqueous solutions by MIEX resin, Chem. Eng. J. 181–182 (2012) 360–370.

[14] P.A. Neale, A.I. Schäfer, Magnetic ion exchange: Is there potential for international development? Desalination 248 (2009) 160–168.

[15] T.H. Boyer, P.C. Singer, A pilot-scale evaluation of magnetic ion exchange treatment for removal of natural organic material and inorganic anions, Water Res. 40 (2006) 2865–2876.

[16] J. Hu, G. Chen, I. Lo, Removal and recovery of Cr(VI) from wastewater by maghemite nanoparticles, Water Res. 39 (2005) 4528–4536.

[17] K.-Y. Shin, J.-Y. Hong, J. Jang, Heavy metal ion adsorption behavior in nitrogen-doped magnetic carbon nanoparticles: Isotherms and kinetic study, J. Hazard. Mater. 190 (2011) 36–44.

[18] Z.Q. Liu, X.M. Yan, M. Drikas, D.N. Zhou, D.S. Wang, M. Yang, J.H. Qu, Removal of bentazone from micro-polluted water using MIEX resin: Kinetics, equilibrium, and mechanism, J. Environ. Sci. 23 (2011) 381–387.

[19] D.A. Fearing, J. Banks, S. Guyetand, C. Monfort Eroles, B. Jefferson, D. Wilson, P. Hillis, A.T. Campbell, S.A. Parsons, Combination of ferric and MIEX® for the treatment of a humic rich water, Water Res. 38 (2004) 2551–2558.

[20] H. Humbert, H. Gallard, H. Suty, J.-P. Croué, Performance of selected anion exchange resins for the treatment of a high DOC content surface water, Water Res. 39 (2005) 1699–1708.

[21] T.H. Boyer, K.C. Graf, S.E.H. Comstock, T.G. Townsend, Magnetic ion exchange treatment of stabilized landfill leachate, Chemosphere 83 (2011) 1220–1227.

[22] L. Ding, C. Wu, H.P. Deng, X.X. Zhang, Adsorptive characteristics of phosphate from aqueous solutions by MIEX resin, J. Colloid Interface Sci. 376 (2012) 224–232.

[23] L. Ding, X. Lu, H.P. Deng, X.X. Zhang, Adsorptive removal of 2,4-Dichlorophenoxyacetic acid (2,4-D) from aqueous solutions using MIEX resin, Ind. Eng. Chem. Res. 51 (2012) 11226–11235.

[24] K. Akhrib, F. Kaouah, T. Berrama, Z. Bendjama, Kinetic and thermodynamic study of removal of o-chlorophenol from potable water using activated carbon prepared by Date Pits, Desalin. Water Treat. 51 (2013) 6049–6057.

[25] I. Özbay, U. Özdemir, B. Özbay, S. Veli, Kinetic, thermodynamic, and equilibrium studies for adsorption of azo reactive dye onto a novel waste adsorbent: Charcoal ash, Desalin. Water Treat. 51 (2013) 6091–6100.

[26] P.S. Koujalagi, S.V. Divekar, R.M. Kulkarni, R.K. Nagarale, Kinetics, thermodynamic, and adsorption studies on removal of chromium(VI) using Tulsion A-27(MP) resin, Desalin. Water Treat. 51 (2013) 3273–3283.

[27] W. Farooq, H.-J. Hong, E.J. Kim, J.-W. Yang, Removal of Bromate (BrO_3^-) from water using cationic surfactant-modified powdered activated carbon (SM-PAC), Sep. Sci. Technol. 47 (2012) 1906–1912.

[28] W.-J. Huang, Y.-L. Cheng, Effect of characteristics of activated carbon on removal of bromate, Sep. Purif. Technol. 59 (2008) 101–107.

[29] A.H. Konsowa, Bromate removal from water using granular activated carbon in a batch recycle, Desalin. Water Treat. 12 (2009) 375–381.

[30] A. Bhatnagar, Y. Choi, Y. Yoon, Y. Shin, B.H. Jeon, J.W. Kang, Bromate removal from water by granular ferric hydroxide (GFH), J. Hazard. Mater. 170 (2009) 134–140.
[31] M.I. Trioni, S. Achilli, E.V. Chulkov, Key ingredients of the alkali atom—Metal surface interaction: Chemical bonding versus spectral properties, Prog. Surf. Sci. 88 (2013) 160–170.
[32] Z.H. Du, M.C. Jia, X.W. Wang, Cesium removal from solution using PAN-based potassium nickel hexacyanoferrate (II) composite spheres, J. Radioanal. Nucl. Chem. 298 (2013) 167–177.
[33] Y.Z. Niu, R.J. Qu, C.M. Sun, C.H. Wang, H. Chen, C.N. Ji, Y. Zhang, X. Shao, F.L. Bu, Adsorption of Pb (II) from aqueous solution by silica-gel supported hyperbranched polyamidoamine dendrimers, J. Hazard. Mater. 244-245 (2013) 276–286.
[34] R.C.I. Fontan, L.A. Minim, R.C.F. Bonomo, L.H.M. da Silva, V.P.R. Minim, Adsorption isotherms and thermodynamics of α-lactalbumin on an anionic exchanger, Fluid Phase Equilib. 348 (2013) 39–44.
[35] W.F. Chen, Z.Y. Zhang, Q. Li, H.Y. Wang, Adsorption of bromate and competition from oxyanions on cationic surfactant-modified granular activated carbon (GAC), Chem. Eng. J. 203 (2012) 319–325.
[36] A. Bhatnagar, M. Sillanpää, Sorption studies of bromate removal from water by nano-Al_2O_3, Sep. Sci. Technol. 47 (2012) 89–95.
[37] R. Chitrakar, K. Mizobuchi, A. Sonoda, T. Hirotsu, Uptake of bromate ion on amorphous aluminum hydroxide, Ind. Eng. Chem. Res. 49 (2010) 8726–8732.
[38] L.A. Wang, J. Zhang, J.Z. Liu, H. He, M. Yang, J.W. Yu, Z.C. Ma, F. Jiang, Removal of bromate ion using powdered activated carbon, J. Environ. Sci. 22 (2010) 1846–1853.
[39] H. Schwegmann, J. Ruppert, F.H. Frimmel, Influence of the pH-value on the photocatalytic disinfection of bacteria with TiO_2-explanation by DLVO and XDLVO theory, Water Res. 47 (2013) 1503–1511.
[40] A. Kilislioglu, B. Bilgin, Thermodynamic and kinetic investigations of uranium adsorption on amberlite IR-118H resin, Appl. Radiat. Isot. 58 (2003) 155–160.
[41] T.Y. Kou, Y.Z. Wang, C. Zhang, J.Z. Sun, Z.H. Zhang, Adsorption behavior of methyl orange onto nanoporous core-shell Cu@Cu_2O nanocomposite, Chem. Eng. J. 223 (2013) 76–83.